Title
Increased cortical porosity in type 2 diabetic postmenopausal women with fragility fractures

Journal
Journal of Bone and Mineral Research, 28(2)

ISSN
0884-0431

Authors
Patsch, Janina M
Burghardt, Andrew J
Yap, Samuel P
et al.

Publication Date
2013-02-01

DOI
10.1002/jbmr.1763

Peer reviewed

Published in final edited form as:
J Bone Miner Res. 2013 February ; 28(2): 313–324. doi:10.1002/jbmr.1763.

Increased Cortical Porosity in Type-2 Diabetic Postmenopausal Women with Fragility Fractures

Janina M. Patsch[1,§], **Andrew J. Burghardt**[1,§], **Samuel P. Yap**[1], **Thomas Baum**[1], **Ann V. Schwartz**[2], **Gabby B. Joseph**[1], and **Thomas M. Link**[1]

[1]Musculoskeletal Quantitative Imaging Research Group, Department of Radiology & Biomedical Imaging, University of California San Francisco, San Francisco, CA USA

[2]Department of Epidemiology and Biostatistics, University of California San Francisco, San Francisco, CA USA

Abstract

The primary goal of this study was to assess peripheral bone microarchitecture and strength in diabetic postmenopausal women with fragility fractures (DMFx) and to compare them with diabetic women without fracture (DM). Secondary goals were to assess differences in non-diabetic women with (Fx) and without fragility fractures (Co) and in women with (DM) and without diabetes (Co).

Eighty women (mean age 61.3±5.7 yrs) were recruited into these groups (n=20 per group). Participants underwent DXA and high-resolution peripheral quantitative computed tomography (HR-pQCT) of the ultradistal and distal radius and tibia. In the HR-pQCT images volumetric bone mineral density, cortical and trabecular structure measures, including cortical porosity, were calculated. Bone strength was estimated using micro-finite element analysis (μFEA). Differential strength estimates were obtained with and without open cortical pores.

At the ultradistal and distal tibia, DMFx had greater intracortical pore volume (+52.6%, p=0.009; +95.4%, p=0.020), relative porosity (+58.1%; p=0.005; +87.9%, p=0.011) and endocortical bone surface (+10.9%, p=0.031; +11.5%, 0.019) than DM. At the distal radius DMFx had 4.7-fold greater relative porosity (p=0.000) than DM. At the ultradistal radius, intracortical pore volume was significantly higher in DMFx than DM (+67.8%, p=0.018). DMFx also displayed larger trabecular heterogeneity (ultradistal radius; +36.8%, p=0.035), and lower total and cortical BMD (ultradistal tibia: −12.6%, p=0.031; −6.8%, p=0.011) than DM. DMFx exhibited significantly higher pore-related deficits in stiffness, failure load and cortical load fraction at the ultradistal and

Corresponding author: Janina M. Patsch, MD, PhD Musculoskeletal Quantitative Imaging Research Group Department of Radiology and Biomedical Imaging University of California, San Francisco 185 Berry St, Suite 350 San Francisco, CA 94158 Tel: +1 (415) 353-9436 Fax: +1 (415) 353-9428 janina.patsch@ucsf.edu.
[§]Authors equally contributed.
Janina M. Patsch janina.patsch@ucsf.edu
Andrew J. Burghardt andrew.burghardt@ucsf.edu
Samuel P. Yap paran.yap@ucsf.edu
Thomas Baum thomas.baum@tum.de
Ann V. Schwartz aschwartz@psg.ucsf.edu
Gabby B. Joseph gabby.joseph@ucsf.edu
Thomas M. Link thomas.link@ucsf.edu

Authors' Roles **Study design:** AJB, AVS, and TML. **Study conduct:** AJB and TML. **Data collection:** SPY, TB, and JMP. **Data analysis:** JMP, SPY, TB, and AJB. **Data interpretation:** AJB, JMP, AVS, GBJ, and TML. **Drafting manuscript:** JMP, AJB, SPY. **Revising manuscript content:** JMP, AJB, AVS, and TML. **Approving final version of manuscript:** JMP, AJB, SPY, TB, GBJ, AVS, and TML. AJB and JMP take responsibility for the integrity of the data analysis.

DISCLOSURES All authors state that they have no conflicts of interest.

distal tibia, and the distal radius than DM. Comparing non-diabetic Fx and Co, we only found a non-significant trend with increase in pore volume (+38.9%, p=0.060) at the ultradistal radius.

The results of our study suggest that severe deficits in cortical bone quality are responsible for fragility fractures in postmenopausal diabetic women.

Keywords

Type-2 Diabetes mellitus; High-Resolution Peripheral Quantitative Computed Tomography; Cortical Porosity; Fragility Fractures; Micro-Finite Element Analysis

Introduction

Type-2 diabetes mellitus is a chronic metabolic disease marked by elevated blood glucose due to impaired glucose metabolism and insulin resistance, that transitions into insulin deficiency over time. While the pathophysiology of diabetic bone disease is largely unknown, multiple cohort studies have shown an increased risk for fragility fractures in postmenopausal women with type-2 diabetes compared to non-diabetic controls, especially at the femur, humerus, and the distal lower extremities (1-3).

The clinical standard for fracture risk assessment is the measurement of areal bone mineral density (aBMD) by Dual-Energy X-ray Absorptiometry (DXA). Although DXA is an effective tool for diagnosing and monitoring various forms of bone loss, there are major limitations especially when applied in patients with complex metabolic bone diseases. Previous studies have found either normal or elevated aBMD in type-2 diabetics, which suggests that their increased fracture risk might be due to other factors that are not captured by aBMD measurements (3-5). Although studies have shown that extra-skeletal factors such as retinopathy, vision loss, and falling, contribute to the increased fracture risk in diabetes, they are not sufficient to explain the discrepancy between DXA and fracture prevalence (6). As a clinical consequence, Schwartz *et al.* have recently pointed out that effective intervention thresholds for fracture prevention in patients with type-2 diabetes might be different than for non-diabetics (7).

High-resolution peripheral quantitative computed tomography (HR-pQCT) has recently emerged as an imaging modality able to characterize three-dimensional cortical and trabecular bone density and micro-architecture of the peripheral skeleton *in vivo* (8). The ability of HR-pQCT to acquire images at spatial resolutions comparable to trabecular dimensions (82 μm) makes it a suitable technique for microstructural analysis of human bone. Several studies have used HR-pQCT to quantitatively assess the geometry, microarchitecture, and biomechanical properties of trabecular bone in individuals of different race (9), gender and age (10-13), and fracture status (8,14-16). Owing to the critical role of cortical bone to the axial load bearing capacity of long bones, several techniques have been proposed to quantify cortical bone structure and porosity from HR-pQCT images (10,17-19). In HR-pQCT imaging, decreases in cortical density and cortical thickness, and increases in cortical porosity are considered surrogate markers for cortical bone loss (10,17). Micro-finite element analysis (μFEA) techniques have been used to calculate estimates of bone strength and load distribution from HR-pQCT scans (20-23). The strength deficit and compartment-specific changes in load distribution associated with cortical porosity can be quantified by differential μFEA modeling (10).

A small number of HR-pQCT studies addressing peripheral bone microarchitecture in type-2 diabetes have been published to date (24,25). While Burghardt *et al.* found higher trabecular BMD and trabecular thickness at the tibia and significantly greater cortical porosity at the

radius, Shu *et al.* reported similar bone microarchitecture in postmenopausal diabetic women versus controls (24,25). Although the first study included a small number of fractured diabetics, neither study specifically recruited diabetic women with fragility fractures. Although evidence of normal to increased bone density and trabecular microarchitecture in diabetics was consistent between these studies, it is currently unclear if diabetics with fragility fractures would present with the same bone phenotypes as non-fracture diabetic cases. Therefore, we have specifically designed this study to quantify cortical and trabecular bone structure and strength in postmenopausal women with type-2 diabetes with and without fragility fractures in comparison with non-diabetic post-menopausal women with and without fragility fractures.

Patients and Methods

Subjects

Eighty postmenopausal women were recruited into one of four groups: type-2 diabetics with fragility fractures (DMFx, n=20), type-2 diabetics without fractures (DM, n=20), non-diabetic women with fragility fractures (Fx, n=20), and healthy (i.e. non-diabetic, non-fracture) controls (Co, n=20). Patients of all study groups were recruited by media outlets including online and newspaper advertisement, flyers, radio announcements and following orthopedic and/or fracture treatment at the University of California, San Francisco (UCSF). The study protocol was approved by the UCSF Committee of Human Research and all patients gave written informed consent before participation.

Inclusion criteria for the entire study population required women to be between 50-75 years old with a body mass index (BMI) between 18 to 37 kg/m^2. All subjects were mobile and able to move without assistance. Subjects recruited into the diabetes groups were required to have a minimum of 3 years history of treatment for type-2 diabetes by oral therapies and/or insulin. Subjects were only included if they sustained a low impact fracture after menopause (DMFx and Fx) and following the onset of diabetes (DMFx cohort only). Patients with pathologic fractures were excluded; pathologic fractures were defined as fractures due to local tumors, tumor-like lesions, or focal demineralization as visualized on radiographs.

Exclusion criteria for all cohorts were as follows: juvenile or premenopausal idiopathic osteoporosis, a history of severe neuropathic disease, recent history of immobilization (>3 months), hyperparathyroidism, hyperthyroidism, immobilization, alcoholism, chronic drug use, chronic gastrointestinal disease, significant chronic renal impairment (CKD stages IV, V), significant chronic hepatic impairment, unstable cardiovascular disease and uncontrolled hypertension as these may potentially have affected bone metabolism. In addition, chronic treatment with antacids, estrogen, rosiglitazone, pioglitazone, adrenal or anabolic steroids, anticonvulsants, anticoagulants, pharmacological doses of vitamin A supplements, fluorides, bisphosphonates, calcitonin, tamoxifen or parathyroid hormone (PTH) were exclusion criteria.

Laboratory Analyses

Fasting blood was drawn between 8 and 11 am. All samples were sent to a Bay Area branch of Quest Diagnostics (Madison, NJ). The test panel included HbA_1c, 25-OH Vitamin D_3, parathyroid hormone (PTH), and serum creatinine. The estimated glomerular filtration rate (eGFR) was calculated according to the MDRD (Modification of Diet in Renal Disease) formula. In African-American women eGFR was corrected for race.

Fracture Confirmation

For all subjects recruited into the fragility fracture groups, previous radiographs were available to document the fracture status. All radiographs were analyzed by a board certified musculoskeletal radiologist (TML) to verify the presence and location of fractures. Radiographs were either available through our institution's Picture Archiving and Communication System (PACS), or they were requested as hard copies or digital images from the study participants. Spine fractures were classified using the standard semi-quantitative scoring system of Genant *et al.* (26). This scoring system differentiates three fracture grades based on the height reduction of the affected vertebral body (grade 1: 20-25%, grade 2: 25-40%, grade 3: >40%).

Dual-Energy X-ray Absorptiometry (DXA)

DXA scans of the lumbar spine (L1-L4), the proximal femur, and the non-dominant distal radius were obtained (Prodigy, GE/Lunar, Milwaukee, WI, USA). Patients were classified as normal, osteopenic, or osteoporotic based on their T-score in accordance with the WHO criteria (27). Quality assurance was performed in accordance with guidelines of the International Society of Clinical Densitometry .

HR-PQCT Imaging

Distal radius and tibia of all patients were scanned on a clinical HR-pQCT scanner (XtremeCT; Scanco Medical AG, Brüttisellen, Switzerland) using the standard *in vivo* protocol (60kVP, 900 μA, 100 ms integration time) as described in the literature (8,12). The standard scan regions are subsequently referred to as the 'ultradistal' location. For both sites, one additional acquisition was performed near the distal margin of the diaphysis with thicker cortical bone to facilitate measurement of cortical bone structure. These scan regions are subsequently referred to as the 'distal' location (Figure 1). Thus, in each patient four peripheral skeletal regions were scanned. Unless the subject reported a history of a local fracture, the non-dominant radius was imaged. In case of a radius fracture history at the non-dominant side, the dominant forearm was imaged. Unless previously fractured, the left tibia was scanned. If the left tibia had been fractured, the contralateral leg was examined.

For the scans, extremities were placed into a carbon fiber cast, which was secured and stabilized. A single antero-posterior scout projection of the scan site was acquired for positioning of the tomographic acquisition. A reference line was placed on the tibial and radial joint surface, respectively; each scan volume spanned 9.02 mm in length (110 slices) and was located at a fixed offset from the reference line (Figure 1). The ultradistal radius scan was offset proximally by 9.5 mm while the ultradistal tibia scan was offset by 22.5 mm. For the exploratory distal diaphyseal scans, the radius and tibia were offset more proximally – 24.5 mm and 37.5 mm with respect to the reference line, for the radius and tibia respectively. For each scan, 750 projections were acquired with a 100 ms integration time. The 126 mm field of view (FOV) was reconstructed across a 1536×1536 matrix, giving an isotropic nominal resolution of 82 μm voxels. Total scan time was 2.8 min for each scan, with each acquisition resulting in an effective dose of approximately 3 μSv. The image attenuation values were calibrated for deriving densitometric bone parameters by a phantom consisting of different concentrations of hydroxyapatite (HA) in a soft-tissue equivalent polymer resin. All scans were graded with regard to motion. Only scans with a scan quality grade 1-3 were used for subsequent image analysis (28).

Image ANALYSIS

Standard Analysis—All scans were analyzed using the manufacturer's standard *in vivo* analysis protocol. The images were semi-automatically segmented using a chaperoned

iterative contouring procedure. All segmentations were monitored for accuracy and were manually modified when contours visually deviated from the periosteal boundary. Densitometric and morphometric parameters were calculated for the trabecular and the cortical compartments (29). The trabecular bone volume fraction (BV/TV) was derived from the BMD of the trabecular compartment (Tb.BMD) using an assumed density for 100% compact mineralized bone (1200 mg HA/cm^3) and background marrow (0 mg HA/cm^3). A Laplace-Hamming filter was used to smooth the image and enhance fine structural details prior to binarization using a fixed threshold (30). Trabecular number (Tb.N) and the standard deviation of inter-trabecular distances (Tb.Sp.SD) were calculated directly using the distance transform method (31) while trabecular thickness (Tb.Th) and separation (Tb.Sp) were derived using plate-model assumptions (32). Cortical thickness was calculated using an annular approximation (29,33).

Cortical Bone Analysis—Extended analysis of the cortical compartment was performed using an automated contouring process and morphologic segmentation of the intra-cortical pore volume (10,34,35). Manual correction of the endosteal contour was performed by a group-blinded operator when the contour erroneously assigned obvious cortical regions to the trabecular compartment (e.g. a large marrow-connected intracortical pore). Cortical porosity was measured using previously described techniques based on the cortical pore volume and mineralized cortical bone volume (10,35). Intracortical pore volume (Ct.Po.V) was calculated as the volume of all voxels identified as intracortical pore space. The intracortical porosity (Ct.Po) was calculated as the ratio of the Ct.Po.V to the total volume of the cortical compartment (intracortical pore and mineralized bone voxels) (10). Additionally, the mean cortical pore diameter (Po.Dm) and the distribution of cortical pore diameters (Po.Dm.SD) were calculated using a distance transformation approach applied to the pore structures (31,35).

Micro-finite element (μFE) analysis—Micro-finite element analysis was applied to the segmented bone structure to evaluate axial bone strength at each site. For each model, the binary image data set was converted to a mesh of isotropic hexahedral elements using a voxel conversion technique (36) and each element was assigned an elastic modulus of 6.829 GPa (20) and a Poisson's ratio of 0.3 (37). Cortical and trabecular bone were labeled as different materials with identical material properties, to facilitate calculation of compartmental load distribution. With fixed nodes at the proximal boundary, a 1% uniaxial compressive strain was applied to the nodes at the distal boundary. The reaction forces at the distal and proximal ends were computed using an iterative solver (Scanco FE Software v1.12; Scanco Medical AG). The axial stiffness (K) was calculated from the reaction force at the boundary and proscribed displacement. The cortical load fraction (Ct.LF) was calculated at the distal boundary as the fraction of the total load applied to cortical bone elements. The failure load (F) was estimated using an optimized criterion described by Mueller *et al.* (22). For the radius, the load to strength ratio (ϕ) was calculated from the failure load estimated by μFEA and the subject-specific fall load predicted for a forward fall on an outstretched forearm (38,39):

$$\text{Load}=550\times\sqrt{2g\times(\text{height}/2)} \quad \text{(Eqn.1)}$$

To estimate the mechanical deficit attributable to the presence of the resolved porosity, a second μFEA simulation was performed for each dataset following artificial removal of all intracortical pore voxels. The difference in stiffness (ΔK_{PO}) and failure load (ΔF_{PO}) between the model with a closed cortex and their respective values from the original model with intact porosity was calculated for each scan and reported as a percent difference. The

difference in the cortical load fraction between the closed and original models, already in units of percent, was simply reported as the absolute difference ($\Delta Ct.LF_{PO}$).

Statistical Analysis

PASW Statistics 18.0 Statistical Database Software (IBM, Armonk, NY) was used for data analysis. For each parameter, data distribution was explored by Shapiro-Wilk tests, inspection of histograms, normal and detrended Q-Q plots and boxplots. Means and standard errors of the mean were calculated for all parameters per group. Group differences in age, height, BMI, HbA_1c, 25-(OH)-vitamin D, PTH, serum creatinine and aBMD were determined by ANOVA and subsequent Tukey-Kramer tests. To address our primary goal, we compared HR-pQCT parameters in the DMFx and DM groups using Mann-Whitney-u-tests or independent samples t-tests as appropriate. In secondary analyses, HR-pQCT parameters in the Co group were compared to the Fx group, and parameters in the DM group were compared to Co group. Due to differences in the racial distributions between Co and Fx as well as Co and DM groups, ANOVA models were used for these comparisons, adjusted for race. Because age was statistically different for Co and Fx groups, these ANOVA models were additionally adjusted for age. As this is the first study exploring bone structure in diabetic women with and without fragility fractures, our purpose is to generate rather than test study hypotheses. In this context, we did not formally adjust for multiple comparisons, but have cautiously interpreted our findings, avoiding over-interpretation of isolated or implausible findings of nominal significance. Statistical significance was defined as $p < 0.05$.

Results

Subject Characteristics

Patient characteristics are presented in Table 1. Comparing DM and DMFx subjects, there were no significant differences in age, height, BMI, HbA_1c, 25-(OH)-vitamin D, PTH, and eGFR levels. DM subjects without fractures had a significantly shorter mean duration of diabetes than DMFx subjects (DM: 8.0 ± 4.9 years; DMFx: 13.3 ± 8.8 years; p=0.025). Non-diabetic Fx subjects were older than Co subjects (p = 0.001) and had higher mean 25-(OH)-vitamin D levels, but there were no other differences between these two groups in mean values of height, BMI, HbA_1c, PTH, and eGFR. Comparing the Co women and the DM women, the two groups without fracture, mean HbA1c levels were significantly higher in diabetics (DM), but none of the other baseline characteristics differed.

The healthy control group (Co) consisted of twelve non-Hispanic Caucasians (60%), five Asians (25%), one African-American (5%), and two Hispanic women (10%). The non-diabetic Fx group consisted of seventeen non-Hispanic Caucasians (85%), two Asians (10%) and one Hispanic (5%). In the diabetic group (DM) without fractures there were seven non-Hispanic Caucasians (35%), seven Asians (35%), four African-Americans (20%), one Hawaiian/Pacific Islander (5%), and one Hispanic (5%). The diabetic group with fragility fractures (DMFx) included eight non-Hispanic Caucasians (40%), six African-Americans (30%), five Asians (25%), and one Hawaiian/Pacific Islander (5%).

Twelve patients had multiple fragility fractures (Fx: n=3; DMFx: n=9), thus the total number of prevalent postmenopausal fragility fractures was 55 (in 40 patients). Specifically, fracture sites for the Fx group included the ankle (n=9), vertebrae (n=6; Grade 1: n=1; Grade 2: n=3; Grade 3: n=2) (26), metatarsals (n=3), humerus (n=2), wrist (n=1), elbow (n=1) and pelvis (n=1). In the DMFx group, fractures sites included ankle (n=7), vertebrae (n=6; Grade 1: n=3; Grade 2: n=2; Grade 3: n=1), metatarsals (n=10), humerus (n=4), wrist (n=2), elbow

(n=1), patella (n=1) , and rib (n=1). All spine fractures in DMFx were clinically non-symptomatic, in the Fx group half of all spine fractures were self-reported.

Areal Bone Density

DXA was performed in 79/80 patients. One patient (DMFx) had severe back pain and was thus not able to tolerate the positioning for DXA. In one Fx subject, the spine results were excluded from statistical analysis due to severe scoliosis. In all four groups, mean T-scores (total hip, spine, and 1/3 radius) were normal to osteopenic (Figure 2). At the spine and the total hip, Fx had significantly lower aBMD than Co (−13.2 %, p = 0.009; −9.0 %, p = 0.024). DMFx had significantly lower total hip aBMD than DM (−7.4 %, p = 0.02). The 1/3 radius site did not yield significant differences between Co versus Fx, DM versus DMFx, or Co versus DM. Co and DM also had similar aBMD at the spine and the total hip.

Peripheral Bone Quality

HR-pQCT was performed in 79/80 patients; in one patient the upper extremity acquisitions were not performed because of a history of bilateral wrist fractures. A small number of scans had to be excluded due to motion artifacts (i.e. visual image quality grade above 3) (28), in total 308 scans (ultradistal radius: 75; ultradistal tibia: 80; distal radius: 74; distal tibia: 79) were available for analyses. Representative images from each of the four groups are presented in Figure 3 (radius) and Figure 4 (tibia). Means and standard deviations of the HR-pQCT-derived parameters and statistical comparisons are provided in Table 2 for the ultradistal and distal radius, and in Table 3 for the ultradistal and distal tibia.

Density and trabecular structure parameters—At both ultradistal scan sites, integral volumetric BMD (BMD) and trabecular bone structure were not significantly different in Co versus Fx and DM versus Co. However, at the ultradistal radius, trabecular heterogeneity was significantly larger in DMFx than in DM (+36.8%; Table 2). At the ultradistal tibia DMFx displayed significantly lower BMD (−12.6%; p=0.031) and cortical BMD (−6.8%; p=0.011) than DM subjects (Table 3).

Cortical bone structure—At the ultradistal radius cortical pore volume was 67.8% greater in DMFx than in DM without fractures (p=0.018). Compared with Co, non-diabetic Fx also exhibited a trend increase in cortical pore volume (+38.9%, (p=0.060) at the ultradistal radius. Although at this scan site, a large difference in relative cortical porosity was found between DMFx and DM, the comparison did not reach statistical significance (+66.9%; p=0.085). Comparing Fx versus Co and DM versus Co, the difference in relative cortical porosity did not reach statistical significance at the ultradistal radius. At the ultradistal radius, the mean pore diameter and the distribution of pore diameters were not different for DMFx versus DM, Fx versus Co, or DM versus Co. Cortical bone structure was comparable in Co and DM.

At the in the ultradistal tibia, cortical porosity was also highest in the DMFx group. DMFx subjects had +52.6% greater Ct.Po.V (p=0.009), relative porosity (+58.1%; p=0.005) and endocortical bone surface (En.BS; +10.9%; p=0.031) than non-fractured DM. In non-diabetics (Fx versus Co), differences in cortical porosity did not reach statistical significance at the ultradistal tibia (+18.4%; p=0.213). Relative cortical porosity was lower in DM than Co but the difference was also not significant.

Similar to the ultradistal tibia, En.BS was greatest at the distal tibia of the DMFx group (+11.5% versus DM; p=0.019). Especially at the distal scan sites, DM without fractures tended to have lower cortical pore volume (radius: −31.3%, p=0.080; tibia: −29.2%, p=0.057), and lower relative cortical porosity than healthy controls (Co; radius: −31.8,

p=0.090; tibia: −29.0%, p=0.052) although differences were not statistically significant. In general, the distal scan sites showed numerically lower levels of cortical porosity than the ultradistal sites. Nevertheless group-specific differences were more pronounced in the distal regions (Table 2 and Table 3). In addition to greater pore volume (radius: 4.7-fold greater, p=0.000; tibia: 2.0-fold greater, p=0.020) and relative cortical porosity (radius: 4.6-fold increase, p=0.000; tibia 1.9 fold greater, p=0.011), DMFx subjects also displayed larger pores (radius: +25.4%, p=0.044; tibia: +13.8%, p=0.020) and a higher variability in pore size (radius: +36.0%, p=0.035; tibia: +19.3%, p=0.019) than DM without fractures. Differences in pore volume and relative porosity at the distal scan sites of non-diabetics (Fx versus Co) were greater at the radius than the tibia but did at neither site reach statistical significance. At both distal radius and distal tibia DM without fractures had the lowest relative cortical porosity of all groups but the differences (versus Co) were not significant.

Bone strength—DMFx tended to have intermediate overall stiffness, failure load, and cortical load fraction and neither of the four scan sites revealed significant differences between DMFx versus DM, Fx versus Co, or DM versus Co. Differential μFEA indices calculated from models computed before and after the artificial closing of the intracortical pores, showed a significant impact of cortical porosity on biomechanical competence. At the distal radius and the distal tibia, DMFx had greater ΔK_{PO} (radius: 5.2-fold greater, p=0.000; tibia: +104%, p=0.016), ΔF_{PO} (radius: 5.3-fold greater, p=0.000; tibia: +108%, p=0.011), and $\Delta Ct.LF_{PO}$ (radius: 3.9-fold greater; +108%, p=0.011) than DM without fractures. In DMFx, significant pore-related biomechanical deficits were also found at the ultradistal tibia when compared with DM (Table 3).

In non-diabetic Fx versus Co subjects there were trends of pore-related deficits in bone strength at all sites with p-values being lowest at the ultradistal radius (ΔK_{PO} −44.4%, p=0.123; ΔF_{PO} −50.8%, p=0.089; $\Delta Ct.LF_{PO}$ −35.1%, p=0.041; Table 2). At both distal scan sites, there were statistical trends towards low pore-related deficits in stiffness (radius: −32.1%, p=0.095; tibia: −26.1%, p=0.084), failure load (radius: −33.3%, p=0.064 ; tibia: −26.3%, p=0.088) and cortical load fraction (radius: −34.9%, p=0.146 ; tibia: −34.3%, p=0.048) in non-fractured DM when compared with Co subjects.

Discussion

Cross-sectional studies and meta-analyses have shown normal to elevated aBMD in patients with type-2 diabetes despite an increased risk of fracture (4,5), leading to the hypothesis that diabetes-associated alterations in bone quality increase fracture risk independent of aBMD (5,25,40). A recent study of postmenopausal women with a history of type-2 diabetes provided the first evidence for macroscopic cortical porosity as the predominant microarchitectural pathomorphology in diabetic bone disease (24). To explicitly investigate whether cortical bone structural impairment is associated with fracture risk in diabetic patients, we designed this cross-sectional case-control study to assess bone quality patterns in diabetics with a history of fragility fracture.

The principal finding of this study was that individuals with type-2 diabetes who have sustained a fragility fracture exhibit significantly greater cortical porosity in the peripheral skeleton than diabetics with no fragility fractures. We did not find a similar association between cortical porosity and fracture in the non-diabetic women although there were trends towards lower bone strength in the control women with prevalent fracture. Interestingly, cortical porosity tended to be lower although not statistically different in non-fractured diabetics than healthy controls. At first glance, these results appear surprising. We hypothesized that 1) those with fracture (i.e. DMFx; Fx) would have greater cortical porosity than control women (i.e. DM; Co) and that 2) women with diabetes (DM) would have

greater porosity than non-diabetic women (Co). Instead, we found evidence that cortical porosity was only strongly related to fracture in those with diabetes and was not a characteristic of diabetes in general. At first glance this appears to contrast our preliminary cross-sectional study on bone quality in type-2 diabetics where we reported that cortical porosity was higher in those with diabetes (24). However, two of the nineteen diabetic patients in this earlier study had a history of fracture, and differences were reduced with the removal of fracture cases which supports our recent finding of significantly different cortical bone quality in DM and DMFx.

Somewhat different from our first study, clear indications of trabecular hypertrophy were absent in the diabetic groups of the present study. However, Shu *et al.* also reported no significant differences in peripheral bone density or trabecular microarchitecture between post-menopausal women with type-2 diabetes and age and race-matched controls (25). Taken altogether, these data suggest relatively well preserved or minimally hypertrophic peripheral bone trabecular microarchitecture in diabetics without fractures and reinforce the notion that intracortical bone loss from cortical porosity is a significant skeletal complication of manifest diabetic bone disease with fractures.

The failure to detect significant differences in bone strength and bone micro-architecture including cortical porosity in the secondary comparisons (i.e. DM versus Co; Fx versus Co) may be due to the relatively small sample size (n=20 per group): Bone strength also tended to be lower in Fx subjects than healthy controls but differences were not significant. At this point in time, reports on cortical porosity in fracture versus non-fracture patients are very limited. Cortical porosity is currently not provided by the standard HR-pQCT software, and only one previous study has considered the relationship between cortical porosity and fracture (19). Although their sample size was much larger, Melton et al. also failed to find significant differences in cortical porosity in postmenopausal fracture versus non-fracture women. Of note, the average age of women in this study was only 62 years, similar to our study. Cortical porosity increases steadily from decade to decade, and women display more accelerated increase in porosity in later menopause (10). Thus, the failure to detect significant differences in non-diabetic Fx versus Co may also be related to the younger age of our patients.

In this study, the DMFx subjects represent a subset of DM patients that are - in spite of similar clinical characteristics compared to the other diabetics - at particularly high fracture risk. The factors that determine cortical porosity are not well understood, but possible contributors include higher levels of advanced glycation endproducts in the bone matrix or even osteocyte dysfunction. Type-2 diabetics typically display low bone turnover (25,41). In addition insulin – which is overtly present because of insulin resistance - is an osteo-anabolic agent. This could also explain why – at a certain point during the earlier stages of the disease - diabetics tend to have higher bone mass, bone mineral density, and lower cortical porosity than non-diabetics. Co-morbidities such as overweight, hypertension or altered lipid metabolism might accumulate over the course of the disease with oxidative stress (42) and other noxae, and cause accelerated aging of various systems including the skeleton. Indeed, when comparing our data with a cross-sectional HR-pQCT study investigating age-related changes in cortical bone quality, we discovered that DMFx subjects exhibited cortical porosity that was not even reached by control subjects in the 8^{th} decade of life (10).

In spite of greatly dichotomous cortical morphology at the extremities, DMFx and DM subjects exhibited highly similar clinical characteristics (Table 1). Kidney function, PTH levels, glycemic control as expressed by HbA_1c, and 25-(OH) vitamin D were comparable between DM and DMFx subjects. Upon chart review, we found that fracture subjects were

more likely to use vitamin supplements, perhaps in response to their fracture history, which may account for the higher vitamin D levels in the Fx subjects.

Another important observation is that greater cortical porosity was concomitant with subject-specific mechanical deficits, particularly in DMFx. Although no differences in overall bone strength were observed in the diabetic cohort with fractures compared to the other cohorts, the differential μFEA results indicated abnormal mechano-structural deficits in the cortical bone of diabetic fracture patients. Particularly the distal (i.e. more cortical) scan sites (Figure 1) demonstrated major deficits in stiffness, failure load, and cortical load fraction as a result of increased cortical porosity in DMFx. On average the porosity-related stiffness deficit in the ultradistal and distal tibia of the DMFx group was almost 10% of the apparent stiffness, representing a disproportionate component of overall bone strength for a small volume of tissue. Together with the general trend of disproportionally high tibial porosity in DMFx and more radial porosity in non-diabetic Fx, this finding seems particularly relevant with regard to the yet unexplained, high incidence of ankle fractures in type-2 diabetics (1). Our study also highlights that differential μFEA is an important contribution to the understanding of metabolic bone diseases with predominantly cortical manifestations such as diabetes mellitus. As seen in this study, estimates of overall bone strength can overlap to a large extent across populations with and without fracture. However the targeted evaluation of the effect of microstructural differences on bone strength using patient-specific differential modeling can detect unique mechano-structural deficits that may be related to fracture risk.

Following the publication of Schnackenburg *et al.*, our analysis is the second *in vivo* study reporting cortical porosity data of two different anatomical bone regions of the same limb (43). In general, diaphyseal regions display lower Ct.Po than ultradistal scan sites, which is consistent with basic anatomy (i.e. thicker, more compact cortex bearing higher axial loads). Especially for comparisons between DM and DMFx, more of the porosity-related parameters yielded significant differences. Nevertheless, it needs to be stressed that at this point in time, ultradistal regions have been established as standard acquisition sites for HR-pQCT imaging (Figure 1). Although the results of our study highlight that HR-pQCT studies investigating cortical bone microstructure should also consider to use distal (i.e. more diaphyseal) scan regions, these exploratory scan sites require additional *in vivo* validation.

Our study has several limitations. First, HR-pQCT measurements were obtained after the occurrence of fractures, and it is possible that cortical porosity is modulated in response to a prevalent fracture. To address this issue, longitudinal studies assessing incident, new fragility fractures in diabetic cohorts examined with HR-pQCT scans are needed. Moreover, type-2 diabetes and diabetic bone disease have a multifactorial etiology. Thus the limited number of subjects and the design of our study were neither able to address the influence of potential covariates such as different types of treatment, or the presence of systemic complications on bone quality nor provide specific pathophysiologic insight into diabetic bone disease. Another limitation of our study is based on the fact that HR-pQCT is a non-invasive technique that cannot assess bone matrix properties. Matrix changes including the accumulation of advanced glycation end products (AGEs) are considered to influence bone strength (44). Diabetes mellitus accelerates the deposition of AGEs in bone, compounding normal age-related changes in the bone matrix. The μFEA technique used in this study to estimate bone strength assumes homogeneous material properties and therefore does not account for tissue-level differences in mineralization or AGE content that may differ among our study groups. Accordingly, as applied here, μFEA may overestimate diabetic bone strength to a certain extent. It is also noteworthy that the current standard μFEA technique for HR-pQCT data only reflects axial loading which is appropriate for simulations of a fall to the outstretched hand but does not address bending strength which might be relevant to

simulate fractures of the lower extremities. As mentioned previously, HR-pQCT can only detect relatively large intracortical pores due to its limited spatial resolution of approximately 130 μm. In addition, it has to be acknowledged that the segmentation of cortical and trabecular bone is certainly complicated by cortical porosity, and endosteal cortical remnants can be difficult to distinguish from adjacent trabecular structures (18). Direct tissue analyses of diabetic human bone would provide insight into more subtle skeletal defects including changes at the matrix/material level. Biopsy analyses (e.g. using micro-computed tomography or synchrotron radiation imaging) would aid in detecting deficits in cortical ultrastructure beyond the limited resolution of HR-pQCT. However, given increased susceptibility to infection and fracture, bone biopsies may not be a viable option for larger scale studies.

In the future, research which combines imaging and bone biology could help to elucidate the pathophysiology of cortical porosity in diabetic bone disease. Bone biomarker data highlight the predominance of low bone turnover in type-2 diabetics (25,41) and a recent publication reported elevated sclerostin levels in type-2 diabetics (45). Extending on these findings, research on diabetic bone disease should aim to investigate bone quality in the light of bone metabolism with a special focus on the mechano-sensing by osteocytes and the wnt/sclerostin/PTH pathway. Understanding which mechanisms drive cortical porosity in diabetics and non-diabetics would be the next step in developing effective therapies for diabetic bone disease.

In conclusion, the results of our study indicate that cortical porosity is significantly higher in diabetic subjects with fragility fractures when compared with non-fractured diabetics. Cortical pores impair bone strength and are likely to contribute to the elevated fracture risk of patients with type-2 diabetes. Because DXA is not able to detect these cortical deficits, HR-pQCT could contribute to future fracture risk refinement in diabetics as well as targeting potential anti-fracture treatments for this population. In order to determine if and to what extent the assessment of cortical porosity might contribute to risk profiling in DM subjects, larger prospective studies are needed to elucidate the important covariates and co-morbidities associated with the pathogenesis and progression of cortical bone abnormalities in this population.

Acknowledgments

The authors thank Thelma Munoz and Melissa Guan for their help in recruiting and consenting the patients, and Prof. Tom Nickolas (Columbia University) for exchange of ideas and his nephrologic input. This study was supported by NIH RC1 AR058405 (to TML), NIH R01 AR060700 (to AJB) and the Erwin-Schrödinger Grant No. J-3079 (Austrian Science Fund; to JMP).

Funding: NIH RC1 AR058405 NIH R01 AR060700 Austrian Science Fund (FWF) Erwin-Schrödinger Grant J-3079

REFERENCES

1. Schwartz AV, Sellmeyer DE, Ensrud KE, Cauley JA, Tabor HK, Schreiner PJ, Jamal SA, Black DM, Cummings SR. Older women with diabetes have an increased risk of fracture: a prospective study. The Journal of clinical endocrinology and metabolism. 2001; 86(1):32–38. [PubMed: 11231974]
2. Janghorbani M, Van Dam RM, Willett WC, Hu FB. Systematic review of type 1 and type 2 diabetes mellitus and risk of fracture. American journal of epidemiology. 2007; 166(5):495–505. [PubMed: 17575306]
3. de L II, van der Klift M, de Laet CE, van Daele PL, Hofman A, Pols HA. Bone mineral density and fracture risk in type-2 diabetes mellitus: the Rotterdam Study. Osteoporosis international : a journal

established as result of cooperation between the European Foundation for Osteoporosis and the National Osteoporosis Foundation of the USA. 2005; 16(12):1713–1720. [PubMed: 15940395]

4. Vestergaard P. Discrepancies in bone mineral density and fracture risk in patients with type 1 and type 2 diabetes--a meta-analysis. Osteoporosis international : a journal established as result of cooperation between the European Foundation for Osteoporosis and the National Osteoporosis Foundation of the USA. 2007; 18(4):427–444. [PubMed: 17068657]
5. Melton LJ 3rd, Riggs BL, Leibson CL, Achenbach SJ, Camp JJ, Bouxsein ML, Atkinson EJ, Robb RA, Khosla S. A bone structural basis for fracture risk in diabetes. The Journal of clinical endocrinology and metabolism. 2008; 93(12):4804–4809. [PubMed: 18796521]
6. Schwartz AV, Hillier TA, Sellmeyer DE, Resnick HE, Gregg E, Ensrud KE, Schreiner PJ, Margolis KL, Cauley JA, Nevitt MC, Black DM, Cummings SR. Older women with diabetes have a higher risk of falls: a prospective study. Diabetes Care. 2002; 25(10):1749–1754. [PubMed: 12351472]
7. Schwartz AV, Vittinghoff E, Bauer DC, Hillier TA, Strotmeyer ES, Ensrud KE, Donaldson MG, Cauley JA, Harris TB, Koster A, Womack CR, Palermo L, Black DM. Association of BMD and FRAX score with risk of fracture in older adults with type 2 diabetes. JAMA. 2011; 305(21):2184–2192. [PubMed: 21632482]
8. Boutroy S, Bouxsein ML, Munoz F, Delmas PD. In vivo assessment of trabecular bone microarchitecture by high-resolution peripheral quantitative computed tomography. The Journal of clinical endocrinology and metabolism. 2005; 90(12):6508–6515. [PubMed: 16189253]
9. Walker MD, Liu XS, Stein E, Zhou B, Bezati E, McMahon DJ, Udesky J, Liu G, Shane E, Guo XE, Bilezikian JP. Differences in bone microarchitecture between postmenopausal Chinese-American and white women. Journal of bone and mineral research : the official journal of the American Society for Bone and Mineral Research. 2011; 26(7):1392–1398. [PubMed: 21305606]
10. Burghardt AJ, Kazakia GJ, Ramachandran S, Link TM, Majumdar S. Age- and gender-related differences in the geometric properties and biomechanical significance of intracortical porosity in the distal radius and tibia. J Bone Miner Res. 2010; 25(5):983–993. [PubMed: 19888900]
11. Macdonald HM, Nishiyama KK, Kang J, Hanley DA, Boyd SK. Age-related patterns of trabecular and cortical bone loss differ between sexes and skeletal sites: a population-based HR-pQCT study. Journal of bone and mineral research : the official journal of the American Society for Bone and Mineral Research. 2011; 26(1):50–62. [PubMed: 20593413]
12. Khosla S, Riggs BL, Atkinson EJ, Oberg AL, McDaniel LJ, Holets M, Peterson JM, Melton LJ 3rd. Effects of sex and age on bone microstructure at the ultradistal radius: a population-based noninvasive in vivo assessment. Journal of bone and mineral research : the official journal of the American Society for Bone and Mineral Research. 2006; 21(1):124–131. [PubMed: 16355281]
13. Dalzell N, Kaptoge S, Morris N, Berthier A, Koller B, Braak L, van Rietbergen B, Reeve J. Bone micro-architecture and determinants of strength in the radius and tibia: age-related changes in a population-based study of normal adults measured with high-resolution pQCT. Osteoporosis international : a journal established as result of cooperation between the European Foundation for Osteoporosis and the National Osteoporosis Foundation of the USA. 2009; 20(10):1683–1694. [PubMed: 19152051]
14. Sornay-Rendu E, Boutroy S, Munoz F, Delmas PD. Alterations of cortical and trabecular architecture are associated with fractures in postmenopausal women, partially independent of decreased BMD measured by DXA: the OFELY study. J Bone Miner Res. 2007; 22(3):425–433. [PubMed: 17181395]
15. Stein EM, Liu XS, Nickolas TL, Cohen A, Thomas V, McMahon DJ, Zhang C, Cosman F, Nieves J, Greisberg J, Guo XE, Shane E. Abnormal microarchitecture and stiffness in postmenopausal women with ankle fractures. The Journal of clinical endocrinology and metabolism. 2011; 96(7): 2041–2048. [PubMed: 21508142]
16. Vico L, Zouch M, Amirouche A, Frere D, Laroche N, Koller B, Laib A, Thomas T, Alexandre C. High-resolution pQCT analysis at the distal radius and tibia discriminates patients with recent wrist and femoral neck fractures. J Bone Miner Res. 2008; 23(11):1741–1750. [PubMed: 18665795]
17. Nishiyama KK, Macdonald HM, Buie HR, Hanley DA, Boyd SK. Postmenopausal women with osteopenia have higher cortical porosity and thinner cortices at the distal radius and tibia than women with normal aBMD: an in vivo HR-pQCT study. Journal of bone and mineral research :

the official journal of the American Society for Bone and Mineral Research. 2010; 25(4):882–890. [PubMed: 19839766]

18. Zebaze RM, Ghasem-Zadeh A, Bohte A, Iuliano-Burns S, Mirams M, Price RI, Mackie EJ, Seeman E. Intracortical remodelling and porosity in the distal radius and post-mortem femurs of women: a cross-sectional study. Lancet. 2010; 375(9727):1729–1736. [PubMed: 20472174]
19. Melton LJ 3rd, Christen D, Riggs BL, Achenbach SJ, Muller R, van Lenthe GH, Amin S, Atkinson EJ, Khosla S. Assessing forearm fracture risk in postmenopausal women. Osteoporosis international : a journal established as result of cooperation between the European Foundation for Osteoporosis and the National Osteoporosis Foundation of the USA. 2010; 21(7):1161–1169. [PubMed: 19714390]
20. Macneil JA, Boyd SK. Bone strength at the distal radius can be estimated from high-resolution peripheral quantitative computed tomography and the finite element method. Bone. 2008; 42(6): 1203–1213. [PubMed: 18358799]
21. Liu XS, Zhang XH, Sekhon KK, Adams MF, McMahon DJ, Bilezikian JP, Shane E, Guo XE. High-resolution peripheral quantitative computed tomography can assess microstructural and mechanical properties of human distal tibial bone. Journal of bone and mineral research : the official journal of the American Society for Bone and Mineral Research. 2010; 25(4):746–756. [PubMed: 19775199]
22. Mueller TL, Christen D, Sandercott S, Boyd SK, van Rietbergen B, Eckstein F, Lochmuller EM, Muller R, van Lenthe GH. Computational finite element bone mechanics accurately predicts mechanical competence in the human radius of an elderly population. Bone. 2011; 48(6):1232–1238. [PubMed: 21376150]
23. Varga P, Baumbach S, Pahr D, Zysset PK. Validation of an anatomy specific finite element model of Colles' fracture. Journal of Biomechanics. 2009; 42(11):1726–1731. [PubMed: 19467661]
24. Burghardt AJ, Issever AS, Schwartz AV, Davis KA, Masharani U, Majumdar S, Link TM. High-resolution peripheral quantitative computed tomographic imaging of cortical and trabecular bone microarchitecture in patients with type 2 diabetes mellitus. J Clin Endocrinol Metab. 2010; 95(11): 5045–5055. [PubMed: 20719835]
25. Shu A, Yin MT, Stein E, Cremers S, Dworakowski E, Ives R, Rubin MR. Bone structure and turnover in type 2 diabetes mellitus. Osteoporos Int. 2011
26. Genant HK, Wu CY, van Kuijk C, Nevitt MC. Vertebral fracture assessment using a semiquantitative technique. Journal of bone and mineral research : the official journal of the American Society for Bone and Mineral Research. 1993; 8(9):1137–1148. [PubMed: 8237484]
27. Assessment of fracture risk and its application to screening for postmenopausal osteoporosis. Report of a WHO Study Group. World Health Organ Tech Rep Ser. 1994; 843:1–129. [PubMed: 7941614]
28. Pialat JB, Burghardt AJ, Sode M, Link TM, Majumdar S. Visual grading of motion induced image degradation in high resolution peripheral computed tomography: Impact of image quality on measures of bone density and micro-architecture. Bone. 2011
29. Laib A, Hauselmann HJ, Ruegsegger P. In vivo high resolution 3D-QCT of the human forearm. Technol Health Care. 1998; 6(5-6):329–337. [PubMed: 10100936]
30. Laib A, Ruegsegger P. Comparison of structure extraction methods for in vivo trabecular bone measurements. Comput Med Imaging Graph. 1999; 23(2):69–74. [PubMed: 10227372]
31. Hildebrand T, Ruegsegger P. A new method for the model-independent assessment of thickness in three-dimensional images. J Microsc-Oxford. 1997; 185:67–75.
32. Laib A, Ruegsegger P. Calibration of trabecular bone structure measurements of in vivo three-dimensional peripheral quantitative computed tomography with 28-microm-resolution microcomputed tomography. Bone. 1999; 24(1):35–39. [PubMed: 9916782]
33. Davis KA, Burghardt AJ, Link TM, Majumdar S. The effects of geometric and threshold definitions on cortical bone metrics assessed by in vivo high-resolution peripheral quantitative computed tomography. Calcified Tissue Int. 2007; 81(5):364–371.
34. Buie HR, Campbell GM, Klinck RJ, MacNeil JA, Boyd SK. Automatic segmentation of cortical and trabecular compartments based on a dual threshold technique for in vivo micro-CT bone analysis. Bone. 2007; 41(4):505–515. [PubMed: 17693147]

35. Burghardt AJ, Buie HR, Laib A, Majumdar S, Boyd SK. Reproducibility of direct quantitative measures of cortical bone microarchitecture of the distal radius and tibia by HR-pQCT. Bone. 2010; 47(3):519–528. [PubMed: 20561906]

36. Muller R, Ruegsegger P. Three-dimensional finite element modelling of non-invasively assessed trabecular bone structures. Medical engineering & physics. 1995; 17(2):126–133. [PubMed: 7735642]

37. Van Rietbergen B, Odgaard A, Kabel J, Huiskes R. Direct mechanics assessment of elastic symmetries and properties of trabecular bone architecture. Journal of biomechanics. 1996; 29(12): 1653–1657. [PubMed: 8945668]

38. Chiu J, Robinovitch SN. Prediction of upper extremity impact forces during falls on the outstretched hand. Journal of biomechanics. 1998; 31(12):1169–1176. [PubMed: 9882050]

39. Melton LJ 3rd, Riggs BL, van Lenthe GH, Achenbach SJ, Muller R, Bouxsein ML, Amin S, Atkinson EJ, Khosla S. Contribution of in vivo structural measurements and load/strength ratios to the determination of forearm fracture risk in postmenopausal women. Journal of bone and mineral research : the official journal of the American Society for Bone and Mineral Research. 2007; 22(9):1442–1448. [PubMed: 17539738]

40. Schwartz AV, Sellmeyer DE. Diabetes, fracture, and bone fragility. Current osteoporosis reports. 2007; 5(3):105–111. [PubMed: 17925191]

41. Pietschmann P, Schernthaner G, Woloszczuk W. Serum osteocalcin levels in diabetes mellitus: analysis of the type of diabetes and microvascular complications. Diabetologia. 1988; 31(12):892–895. [PubMed: 3266486]

42. Frassetto LA, Sebastian A. How metabolic acidosis and oxidative stress alone and interacting may increase the risk of fracture in diabetic subjects. Med Hypotheses. 2012; 79(2):189–192. [PubMed: 22583559]

43. Schnackenburg KE, Macdonald HM, Ferber R, Wiley JP, Boyd SK. Bone Quality and Muscle Strength in Female Athletes with Lower Limb Stress Fractures. Med Sci Sports Exerc. 2011; 43(11):2110–2119. [PubMed: 21552163]

44. Yamagishi SI. Role of advanced glycation end products (AGEs) in osteoporosis in diabetes. Curr Drug Targets. 2011

45. Garcia-Martin A, Rozas-Moreno P, Reyes-Garcia R, Morales-Santana S, Garcia-Fontana B, Garcia-Salcedo JA, Munoz-Torres M. Circulating levels of sclerostin are increased in patients with type 2 diabetes mellitus. The Journal of clinical endocrinology and metabolism. 2012; 97(1):234–241. [PubMed: 22031520]

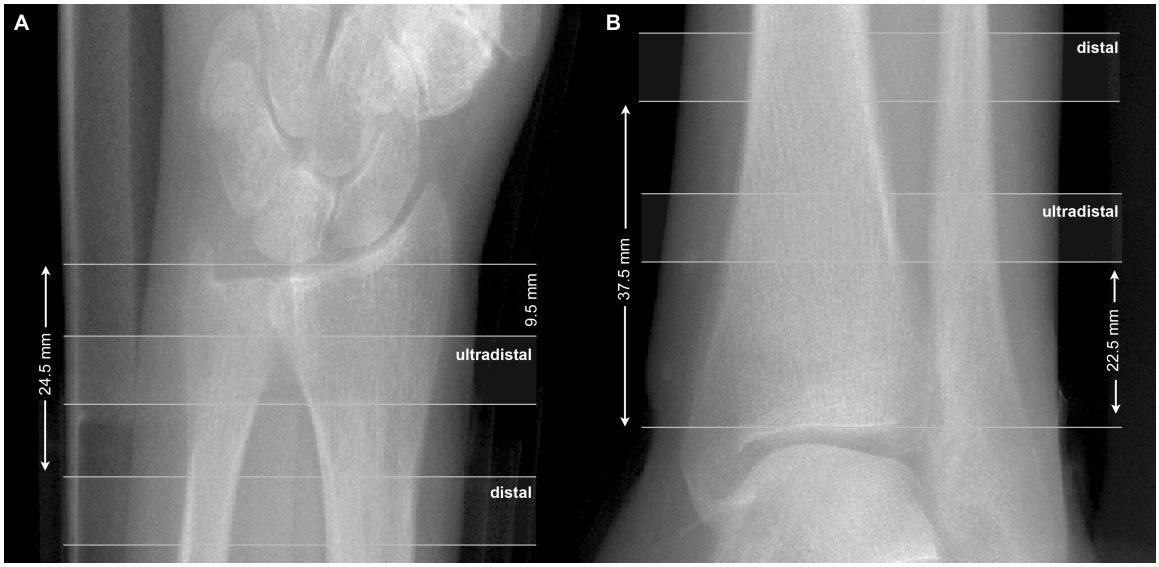

Figure 1.
Scout radiographs of the distal radius (A) and tibia (B), illustrating the standard ultradistal and exploratory distal scan regions.

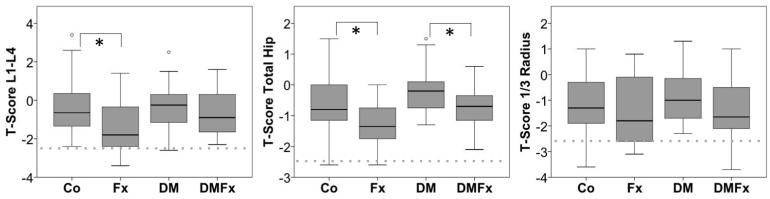

Figure 2. Boxplots of DXA measurements of the lumbar spine (L1-L4), total hip, and the 1/3 radius for all groups

Co = Controls, Fx = Non-diabetic fracture patients, DM = diabetic patients without fractures, DMFx = diabetic patients with fractures. Dotted line indicates diagnostic threshold for osteoporosis (T-Score < 2.5). Asterisks represent significant group differences.

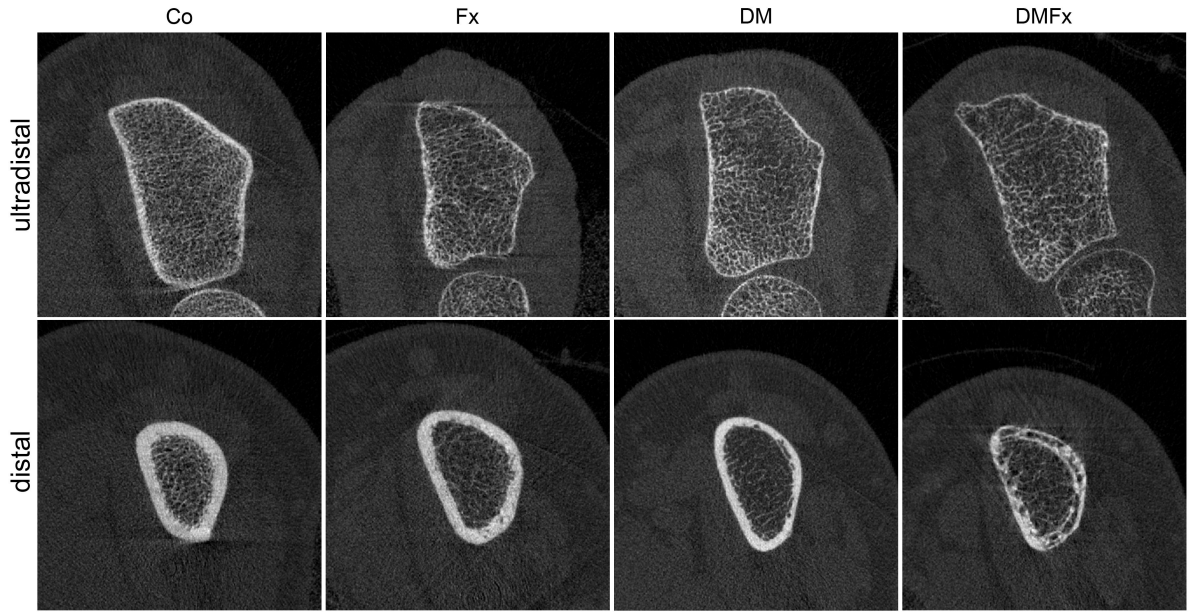

Figure 3. Representative HR-pQCT images of the ultradistal (above) and distal (below) *radius*
shown are the mid-stack tomograms for the Co (left), Fx (left-center), DM (right-center), and DMFx (right) groups. Major cortical porosity can be seen in DMFx (right).

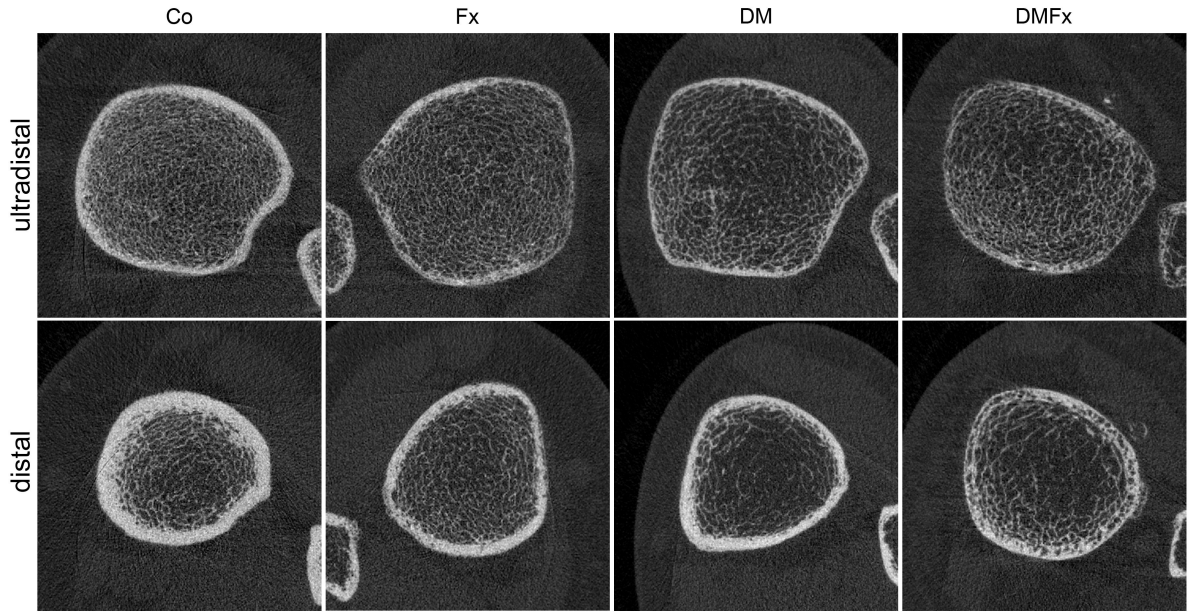

Figure 4. Representative HR-pQCT images of the ultradistal (above) and distal (below) *tibia*
shown are the mid-stack tomograms for the Co (left), Fx (left-center), DM (right-center), and DMFx (right) groups. Major cortical porosity can be seen in DMFx (right).

Table 1

Descriptive data of all study participants

Data are expressed as mean ± SEM. eGFR (estimated glomerular filtration rate) is expressed as median [25th-75th percentile].

	CO (n=20)	Fx (n=20)	DM (n=20)	DMFx (n=20)
Age (yr)	58.0 ± 1.1 *a*	64.5 ± 1.3 *a*	59.6 ± 0.9	63.3 ± 1.3
Height (cm)	162.0 ± 1.3	162.0 ± 1.8	159.7 ± 1.6	160.0 ± 1.5
BMI (kg/m^2)	26.0 ± 1.0	25.3 ± 0.8	27.8 ± 0.8	28.9 ± 1.2
HbA1c (%)	5.8 ± 0.1 *c*	5.9 ± 0.1	7.9 ± 0.3 *c*	7.9 ± 0.6
25-(OH) Vitamin D (ng/ml)	28.6 ± 11.4 *a*	42.1 ± 11.4 *a*	27.4 ± 11.5	32.7 ± 12.7
PTH (pg/ml)	37.3 ± 14.0	33.5 ± 23.8	38.4 ± 15.8	41.4 ± 25.5
eGFR ml/min/1.73 m^2	87.8 [77.3 – 98.0]	83.5 [69.0 – 86.3]	98.1 [76.8 – 117.0]	89.3 [69.2 – 101.7]

a = $p < 0.05$ CO versus Fx,

b $p < 0.05$ DM versus DMFx,

c $p < 0.05$ CO versus DM.

Table 2

Standard parameters, cortical porosity, and biomechanical parameters of the ultradistal and distal radius for all groups

Data are expressed as mean ± SEM. Boldface indicates significant difference:

	CO (n=20)	Fx (n=20)	DM (n=20)	DMFx (n=20)
Ultradistal Radius	Non-Diabetic		Diabetic	
Basic HR-pQCT measures				
Tt.Ar (mm^2)	269 ± 12	261 ± 10	252 ± 12	258 ± 13
BMD (mg HA/cm^3)	281 ± 15	261 ± 12	299 ± 13	282 ± 17
Tb.BMD (mg HA/cm^3)	146 ± 10	136 ± 7	151 ± 7	146 ± 8
Ct.BMD (mg HA/cm^3)	827 ± 14	785 ± 16	834 ± 17	793 ± 21
Ct.Th (mm)	0.64 ± 0.04	0.58 ± 0.04	0.68 ± 0.04	0.63 ± 0.05
Tb.N (1/mm)	1.77 ± 0.09	1.78 ± 0.05	1.90 ± 0.06	1.77 ± 0.07
Tb.Sp.SD (mm)	0.28 ± 0.06	0.24 ± 0.02	0.20 ± 0.08	**0.26 ± 0.03** *
Porosity				
Ct.PoV (mm^3)	10.40 ± 1.62	14.44 ± 1.51	11.00 ± 1.60	**18.46 ± 3.85** *
Ct.Po (%)	2.37 ± 0.37	3.52 ± 0.33	2.54 ± 0.37	4.24 ± 1.00
Po.Dm (mm)	0.17 ± 0.01	0.18 ± 0.01	0.17 ± 0.01	0.18 ± 0.01
Dm.SD (mm)	0.07 ± 0.00	0.08 ± 0.01	0.07 ± 0.00	0.08 ± 0.01
En.BS (mm^2)	594 ± 16	588 ± 15	563 ± 17	591 ± 18
Biomechanics				
Stiffness, K (kN/mm)	43.7 ± 2.2	38.1 ± 1.8	43.4 ± 2.0	41.0 ± 1.9
Failure Load, F (N)	2610 ± 126	2287 ± 102	2580 ± 110	2450 ± 106
ϕ, load/strength ratio	0.87 ± 0.04	1.00 ± 0.05	0.87 ± 0.03	0.92 ± 0.04
Ct.LF distal (%)	48.7 ± 1.6	50.0 ± 1.9	51.1 ± 1.9	48.7 ± 1.7
Differential Biomechanics				
ΔK_{PO} (%)	2.30 ± 0.42	3.32 ± 0.30	2.59 ± 0.42	4.04 ± 0.91
ΔF_{PO} (%)	1.70 ± 0.32	2.57 ± 0.27	1.95 ± 0.36	3.07 ± 0.72
$\Delta Ct.LF_{PO}$ (%)	1.07 ± 0.14	**1.44 ± 0.16** δ	1.31 ± 0.18	1.39 ± 0.14
Distal Radius	**Non-Diabetic**		**Diabetic**	
Porosity				
Ct.PoV (mm^3)	6.82 ± 0.98	14.06 ± 5.80	4.69 ± 0.71	**22.06 ± 13.31** *
Ct.Po (%)	1.22 ± 0.19	2.46 ± 0.99	0.83 ± 0.13	**3.86 ± 1.30** *
Po.Dm (mm)	0.17 ± 0.01	0.19 ± 0.01	0.17 ± 0.01	**0.22 ± 0.02** *
Dm.SD (mm)	0.07 ± 0.00	0.08 ± 0.01	0.07 ± 0.01	**0.10 ± 0.01** *
En.BS (mm^2)	325 ± 13	314 ± 10	296 ± 14	321 ± 12
Biomechanics				
Stiffness, K (kN/mm)	51.9 ± 2.1	50.6 ± 2.1	51.0 ± 1.8	49.4 ± 2.1

	CO (n=20)	Fx (n=20)	DM (n=20)	DMFx (n=20)
Failure Load, F (N)	2896 ± 116	2818 ± 118	2860 ± 100	2746 ± 117
Ct.LF distal (%)	0.91 ± 0.95	0.93 ± 0.83	0.91 ± 1.12	0.90 ± 0.91
Differential Biomechanics				
ΔK_{PO} (%)	1.63 ± 0.25	3.68 ± 1.70	1.11 ± 0.18	**5.75 ± 2.33** *
ΔF_{PO} (%)	1.64 ± 0.24	3.69 ± 1.69	1.10 ± 0.17	**5.80 ± 2.34** *
$\Delta Ct.LF_{PO}$ (%)	0.19 ± 0.04	0.26 ± 0.08	0.13 ± 0.02	**0.50 ± 0.17** *

*DM vs. DMFx.

§Co vs. Fx.

#DM vs. Co.

Table 3

Standard parameters, cortical porosity, and biomechanical parameters of the ultradistal and distal tibia for all groups

Data are expressed as mean ± SEM. Boldface indicates significant difference:

	Co (n=20)	Fx (n=20)	DM (n=20)	DMFx (n=20)
Ultradistal Tibia	Non-Diabetic		Diabetic	
Basic HR-pQCT measures				
Tt.Ar (mm^2)	681 ± 27	682 ± 25	607 ± 32	667 ± 24
BMD (mg HA/cm^3)	272 ± 13	255 ± 14	298 ± 10	**261 ± 13** *
Tb.BMD (mg HA/cm^3)	156 ± 9	151 ± 6	164 ± 5	153 ± 8
Ct.BMD (mg HA/cm^3)	825 ± 14	786 ± 18	849 ± 15	**791 ± 16** *
Ct.Th (mm)	1.03 ± 0.06	0.92 ± 0.07	1.09 ± 0.05	0.96 ± 0.07
Tb.N (1/mm)	1.77 ± 0.09	1.67 ± 0.06	1.70 ± 0.08	1.65 ± 0.09
Tb.Sp.SD (mm)	0.24 ± 0.02	0.30 ± 0.03	0.24 ± 0.01	0.30 ± 0.04
Porosity				
Ct.PoV (mm^3)	66.89 ± 5.97	74.84 ± 8.68	59.97 ± 7.94	**91.54 ± 10.83** *
Ct.Po (%)	7.06 ± 0.62	8.35 ± 0.69	6.21 ± 0.72	**9.82 ± 1.08** *
Po.Dm (mm)	0.19 ± 0.00	0.20 ± 0.00	0.20 ± 0.01	0.21 ± 0.01
Dm.SD (mm)	0.09 ± 0.00	0.09 ± 0.00	0.09 ± 0.00	0.10 ± 0.00
En.BS (mm^2)	843 ± 22	851 ± 20	783 ± 25	**868 ± 28** *
Biomechanics				
Stiffness, K (kN/mm)	121.3 ± 4.4	113.2 ± 3.8	120.9 ± 3.2	118.0 ± 5.8
Failure Load, F (N)	7017 ± 255	6575 ± 209	6943 ± 190	6811 ± 334
Ct.LF distal (%)	48.6 ± 2.2	45.0 ± 2.3	49.8 ± 2.1	46.0 ± 1.9
Differential Biomechanics				
ΔK_{PO} (%)	6.86 ± 0.72	7.74 ± 0.81	5.98 ± 0.79	**9.13 ± 1.14** *
ΔF_{PO} (%)	5.88 ± 0.65	6.60 ± 0.75	5.19 ± 0.70	**7.73 ± 0.96** *
$\Delta Ct.LF_{PO}$ (%)	3.18 ± 0.27	3.48 ± 0.31	3.06 ± 0.36	**4.18 ± 0.38** *
Distal Tibia	Non-Diabetic		Diabetic	
Porosity				
Ct.PoV (mm^3)	52.45 ± 7.44	53.61 ± 7.25	37.12 ± 4.83	**72.51 ± 13.3** *
Ct.Po (%)	4.27 ± 0.61	4.75 ± 0.73	3.03 ± 0.39	**5.70 ± 0.80** *
Po.Dm (mm)	0.18 ± 0.01	0.19 ± 0.01	0.18 ± 0.01	**0.20 ± 0.01** *
Dm.SD (mm)	0.08 ± 0.00	0.09 ± 0.00	0.08 ± 0.00	**0.10 ± 0.01** *
En.BS (mm^2)	638 ± 18	643 ± 18	593 ± 21	**661 ± 18** *
Biomechanics				

	Co (n=20)	Fx (n=20)	DM (n=20)	DMFx (n=20)
Stiffness, K (kN/mm)	129.1 ± 4.7	117.0 ± 3.8	123.7 ± 2.3	120.0 ± 5.4
Failure Load, F (N)	7195 ± 266	6515 ± 212	6879 ± 137	6666 ± 310
Ct.LF distal (%)	76.83 ± 1.91	77.64 ± 1.66	78.89 ± 1.50	75.91 ± 1.61
Differential Biomechanics				
ΔK_{PO} (%)	5.28 ± 0.69	5.99 ± 0.86	3.90 ± 0.52	**7.97 ± 1.59** *
ΔF_{PO} (%)	4.93 ± 0.66	5.61 ± 0.80	3.64 ± 0.49	**7.58 ± 1.54** *
$\Delta Ct.LF_{PO}$ (%)	1.38 ± 0.23	1.50 ± 0.26	**0.91 ± 0.13** #	**1.88 ± 036** *

* DM vs. DMFx.

§ Co vs. Fx.

DM vs. Co.